Metabolites of the Angiotensin II Antagonist Tasosartan: The Importance of a Second Acidic Group

John W. Ellingboe,* Michael D. Collini, Dominick Quagliato, James Chen, Madelene Antane, Jean Schmid, Dale Hartupee, Valerie White, C. Hyung Park, Tarak Tanikella, and Jehan F. Bagli

Divisions of Chemical Sciences, Cardiovascular and Metabolic Disorders, and Structural Biology, Wyeth-Ayerst Research, CN 8000, Princeton, New Jersey 08543, and 401 North Middletown Road, Pearl River, New York 10965

Received April 17, 1997

Described in this paper is the synthesis and pharmacological activity of five metabolites of the angiotensin II antagonist tasosartan (**1**). Of particular interest is the effect of the additional acidic group of the enol metabolite (**8**) on activity. As suggested by the structural−activity relationship of other angiotensin II antagonist series, a second acidic group can improve receptor binding activity but decrease in vivo activity after oral dosing. The metabolic introduction of a second acidic group in tasosartan bypasses this problem and contributes to the excellent profile of the compound. A molecular modeling study provides a rationale for the role of the enol group of **8** in AT_1 receptor binding.

The renin−angiotensin system (RAS) plays an important role in the regulation of blood pressure through the actions of angiotensin II (A II) (vasoconstriction, aldosterone secretion, renal sodium reabsorption, and norepinephrine release) and thus is an appropriate target for therapeutic intervention in hypertension.[1] Inhibition and antagonism of the various components of the RAS have been the subject of extensive research, culminating in such drugs as angiotensin converting enzyme (ACE) inhibitors,[2] renin inhibitors,[3] and more recently A II antagonists.[4]

Many reported A II antagonists have a tetrazole group which is of particular importance for potency and oral bioavailability. In addition, most of these antagonists have a group which can act as a hydrogen bond acceptor, such as a heterocyclic nitrogen, or as a hydrogen bond donor, such as a hydroxy group or a carboxylic acid (Chart 1). In particular, a second acidic group appears to make a significant contribution to AT_1 receptor binding. However, this second acidic group can have detrimental effects on oral bioavailability. For example, the Glaxo compound GR117289 (**5**) was found to have only 20% bioavailability in humans due to poor absorption, which was attributed to the fact that the compound is a diacid.[5] A prodrug approach has been used to mask the carboxylic acid groups in elisartan (**4**),[6] a prodrug of EXP3174 (**3**), and candesartan (**6**).[7] In the case of losartan (**2**), a carboxylic acid is introduced metabolically through oxidation of the hydroxymethyl group, to yield EXP3174 (**3**).[8] The AT_1 receptor IC_{50} improves from 19 nM to 1.3 nM with the second acidic group.[1] However, oral bioavailability in rats decreases from 33% for losartan (**2**) to 12% for EXP3174 (**3**).[9] In normotensive rats, EXP3174 (**3**) is 15 times more potent than losartan by the IV route, but is less potent after oral administration.[10]

Tasosartan (**1**) is a potent, orally active A II antagonist with a tetrazole ring and a heterocyclic nitrogen

Chart 1

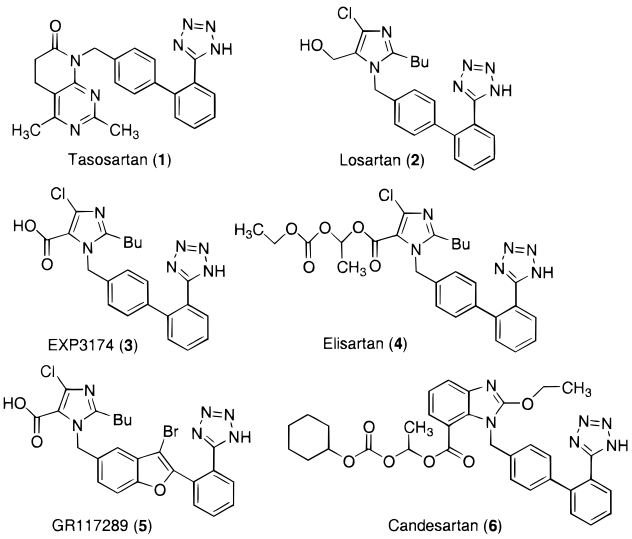

that may serve as a hydrogen bond acceptor, but lacking a second acidic group. In Goldblatt (2K-1C) hypertensive rats, **1** is 30 times more potent than losartan (**2**) after intragastric dosing.[11] The metabolic fate of **1** has been studied; four metabolites were identified in rats, and a fifth metabolite was found in man (Chart 2).[12] The 5-hydroxy compound (**7**) and the enol compound (**8**) were isolated from rat urine, and the unsaturated compound (**9**) and the tetrazole N-2 glucuronide (**10**) were found in rat bile. Compounds **7**, **8**, and **9** were also identified in rat plasma. A hydroxylated enol metabolite (**11**) was identified in human plasma, as were **7**, **8**, and **9**. The enol in compounds **8** and **11** is relatively acidic, and this functional group appears to play an important role in binding to the AT_1 receptor. The synthesis and pharmacology of these metabolites is described in this paper. Also, the role of the enol group of compounds **8** and **11** in binding to the AT_1 receptor is discussed.

* Corresponding author. Current address: Wyeth-Ayerst Research, 401 N. Middletown Rd., Pearl River, NY 10965.

10.1021/jm970690q CCC: $15.00
Published on Web 09/24/1998

Chart 2

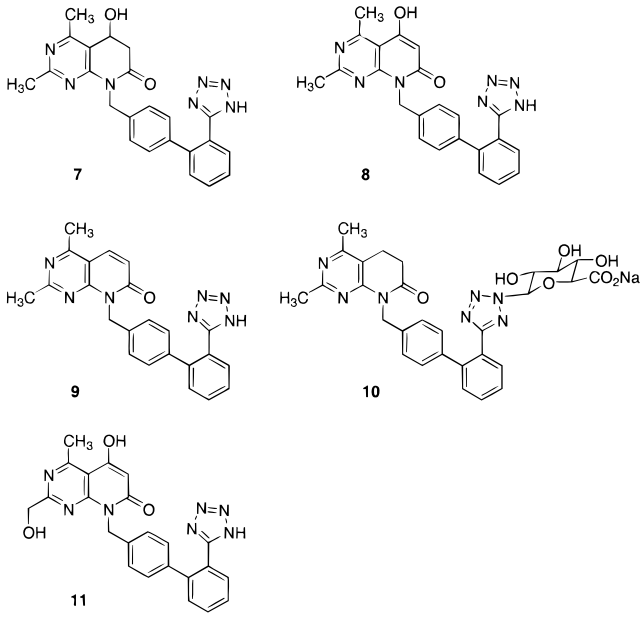

Scheme 1

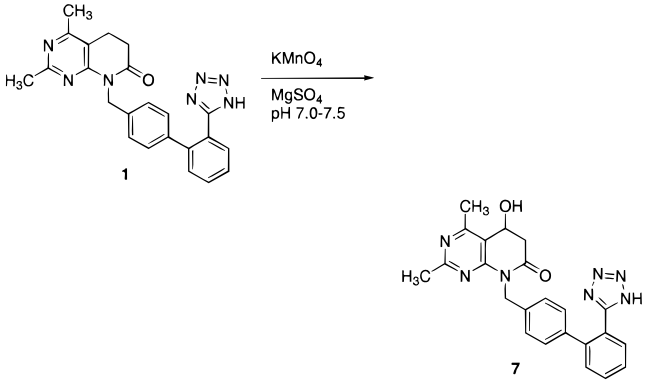

Chemistry

Metabolites **7** and **10** were synthesized directly from compound **1** (Schemes 1 and 2). Thus, oxidation of **1** with $KMnO_4$ gave the hydroxy metabolite (**7**) in a yield of 8%. The N-2 glucuronide (**10**) was prepared in three steps from **1**. Glycosidation of the tetrazole potassium salt of **1** with bromo-2,3,4-tri-*O*-acetyl-α-D-glucopyranuronic acid methyl ester gave 34% of the N-2 glucuronide (**12a**) and 18% of the N-1 glucuronide (**12b**). Removal of the glucuronide acetate groups of **12a** with KCN in MeOH yielded methyl ester **13** (63% yield), and hydrolysis of the methyl ester with 1 N NaOH in MeOH gave the glucuronide (**10**) (62% yield).

The enol metabolite (**8**) was synthesized in eight steps from 2,6-dimethyl-4-hydroxypyrimidine (Scheme 3). Iodination and chlorination with phosphorus oxychloride yielded **15**, which was coupled with (1-ethoxyvinyl)-tributyltin to give pyrimidine **16**. Reaction of **16** with 4-bromobenzylamine and hydrolysis of the enol ether yielded 5-acetylpyrimidine **18**. Palladium-catalyzed coupling of **18** with 2-[(2-*tert*-butyl)-2*H*-tetrazol-5-yl]-phenylboronic acid[11] gave compound **19**. The pyrido ring was introduced by reaction of **19** with diethyl carbonate, and the *tert*-butyl protecting group on the tetrazole of **20** was removed with trifluoromethanesulfonic acid in refluxing toluene to yield the enol metabolite (**8**). None of the keto tautomer is observed in the NMR spectrum.

Determination of the pK_a of the enol group of **8** was attempted, but the low solubility of the compound complicated the experiment. Therefore, intermediate **20** was examined, and a pK_a value of 9.73 ± 0.37 for the enol group was determined by potentiometric titration. Since the only difference between **8** and **20** is the *tert*-butyl protecting group on the tetrazole, the pK_a values for the enols in compounds **8** and **11** are expected to be very close to the value determined for **20**.

The hydroxyenol metabolite (**11**) was prepared by a similar route to compound **8**, but introduction of the hydroxy group required four additional steps (Scheme 4). Methoxyacetonitrile (**23**) was converted into methoxyacetamidine (**25**) and then reacted with ethyl acetoacetate to yield pyrimidine **26**. Iodination, chlorination, and coupling with (1-ethoxyvinyl)tributyltin gave ethoxyvinylpyrimidine **29**. In contrast to the enol (**8**) synthesis, the whole biphenyl tetrazole was incorporated in one piece. Thus, reaction of **29** with 2′-(2-*tert*-butyl-2*H*-tetrazole-5-yl)-4-methylaminobiphenyl (**35**) (prepared according to Scheme 5, by reduction of the nitrile in compound **34** to an amine) yielded compound **30**, which was hydrolyzed to acetylpyrimidine **31**. Cyclization with diethyl carbonate gave **32**, which was deprotected in two steps. The methyl group was removed with BBr_3 and the *tert*-butyl group was removed with trifluoromethanesulfonic acid to give the hydroxyenol metabolite (**11**).

Metabolite **9**, the unsaturated analogue of **1**, was synthesized from pyridopyrimidine **21** (prepared according to Sakamoto[13]). Alkylation of **21** with 2-[4-(bromomethyl)phenyl]benzonitrile yielded **22**, and conversion of the nitrile into a tetrazole with NaN_3/*n*-Bu_3SnCl gave metabolite **9** (Scheme 6).

In Vitro Binding

The metabolites (**7**−**11**) were tested for the inhibition of [^{125}I]A II binding in either a rat adrenal or liver membrane preparation. Results are listed in Table 1. The IC_{50} for compound **1** is 1.20 nM (adrenal membrane). The introduction of a 5-hydroxy group as in metabolite **7** does not have a large effect (IC_{50} = 2.30 nM, adrenal membrane), and the unsaturated metabolite **9** is only slightly less potent than **1** (IC_{50} = 6.50 nM, liver membrane). Glucuronidation takes place at the tetrazole N-2 position and the resulting glucuronide **10** does not inhibit binding of A II at 100 nM (liver membrane). The remaining two compounds, **8** and **11**, contain the enol group and are the most potent compounds in the binding assay, with IC_{50} values of 0.17 and 0.41 nM (adrenal membrane), respectively. Since the hydroxy metabolite **7** does not show a similar increase in potency, the relative acidity of the enol group appears to contribute to the enhanced binding. The increase in binding affinity (∼1 order of magnitude) after the metabolic introduction of the enol group in **8** parallels the increase observed for the carboxylic acid metabolite (**3**) of losartan (**2**). A model for the contribution of the enol to AT_1 receptor binding is discussed below.

Scheme 2

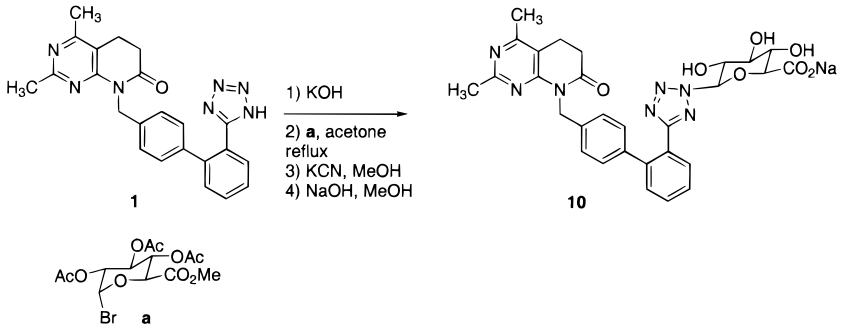

Scheme 3

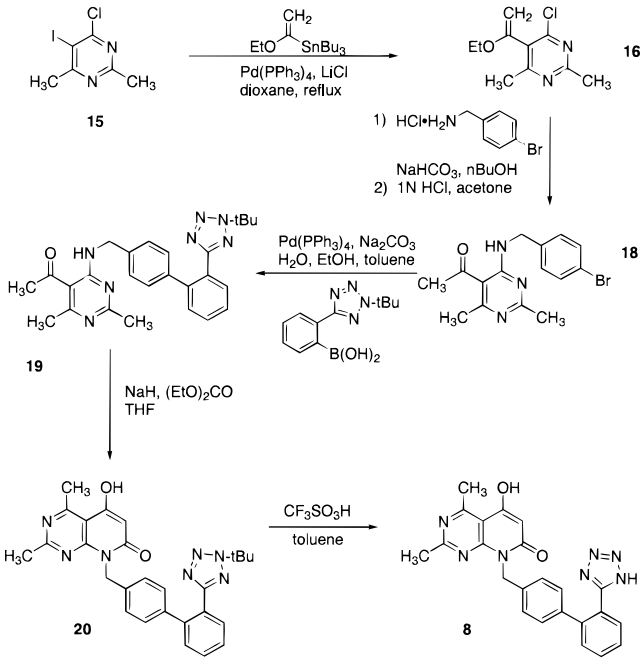

In Vivo Testing

Compounds **1**, **7**, and **8** were tested in Goldblatt (2K-1C) hypertensive rats (**11** was identified later in clinical trials and never tested in the model). In this model the left renal artery of normotensive rats is constricted by a silver clip. The resultant hypertension is associated with an elevated plasma renin activity and increased circulating and/or tissue levels of A II. Mean arterial pressure (MAP) was monitored for 24 h, and the maximum decrease in MAP after various intragastric (ig) and intravenous (iv) doses is reported for all three compounds in Table 2 and in Figures 1−3. Figures 1 and 3 are plotted on a log scale because of the large dose ranges, but the *x*-axis in Figure 2 is linear. The maximum decrease in MAP is approximately the same for all compounds and for both routes of administration (within the normal range of biological variability for the model), but the therapeutic doses vary significantly. The therapeutic dose is the minimum dose to produce the maximum decrease in MAP.

Compound **1** was initially tested ig over a large dose range (0.1−30.0 mg/kg, Table 2, Figure 1). However, as the potency of **1** became apparent, subsequent analogues and metabolites were tested over a narrower dose range, as seen with the remaining entries in Table 2. Compound **1** has a therapeutic dose of 1.0 mg/kg after both ig and iv dosing. At this dose, the decreases in MAP were 71 ± 14 (ig) and 53 ± 10 (iv) mmHg. Higher doses do not produce significantly larger decreases in MAP. For compound **7**, ig doses of 1.0, 3.0, and 10.0 mg/kg produced similar decreases in MAP of 55 ± 15, 54 ± 10, and 71 ± 11 mmHg (Table 2, Figure 2), so the ig therapeutic dose is 1.0 mg/kg. Intravenous doses of 1.0, 3.0, and 10.0 mg/kg of **7** also produced similar decreases of 51 ± 13, 47 ± 15, and 41 ± 8 mmHg (Table 2, Figure 2), giving a therapeutic dose of 1.0 mg/kg. The ig therapeutic dose for compound **8** is 10.0 mg/kg (66 ± 12 mmHg decrease), and the iv therapeutic dose is 0.10 mg/kg (67 ± 11 mmHg decrease) (Table 2, Figure 3). These doses are an order of magnitude higher than the ig therapeutic dose of **1** and an order of magnitude lower than the iv therapeutic dose for **1**, respectively. This difference in iv therapeutic doses for **1** and **8** reflects their difference in potency in the AT_1 binding assay. The 100-fold difference in the ig and iv therapeutic doses for **8** (Figure 3) suggests that **8** is not absorbed as well as **1** after oral administration.

Compound **8** is a major metabolite in mouse, rat, and monkey plasma (but is not detected in dog plasma)[12] as well as in human plasma. In male rats, after oral administration of a single dose of ^{14}C-tasosartan (1.0 mg/kg), the metabolites were present in the plasma to the following extent (% radioactivity in plasma) at 1 h: (**1**) 50%, (**7**) 14%, (**8**) 30%, and (**11**) not detected. The percentage of radioactivity in plasma at 7 h was (**1**) 4%, (**7**) 10%, (**8**) 76%, and (**11**) not detected.[12] The metabolic pathway for the plasma metabolites was elucidated as follows: **1** is hydroxylated to give **7**, which is further oxidized to give **8** and then **11**.[12] Thus, the in vivo data reported in Table 2 and Figures 1−3 for compounds **1** and **7** reflects activity due to multiple species (**1**, **7**, and **8**). Compound **8** is more slowly eliminated than **1** or **7**[12] and appears to be the major contributor to the biological activity of tasosartan. It is fortunate that compound **1** is metabolized to produce **8**, since the latter compound does not appear to be well absorbed after oral administration yet is far more potent than **1**.

Modeling Studies

Since the enolic group of **8** appears to be essential for the increase in potency over **1**, modeling studies were carried out to determine a role for the enol in receptor binding. Based on published homology[14] and 3D pharmacophore[15] studies depicting the possible bound conformations of AT_1 antagonists, molecular models of tasosartan (**1**) and the enol metabolite (**8**) were compared with models for losartan (**2**) and its metabolite

Scheme 4

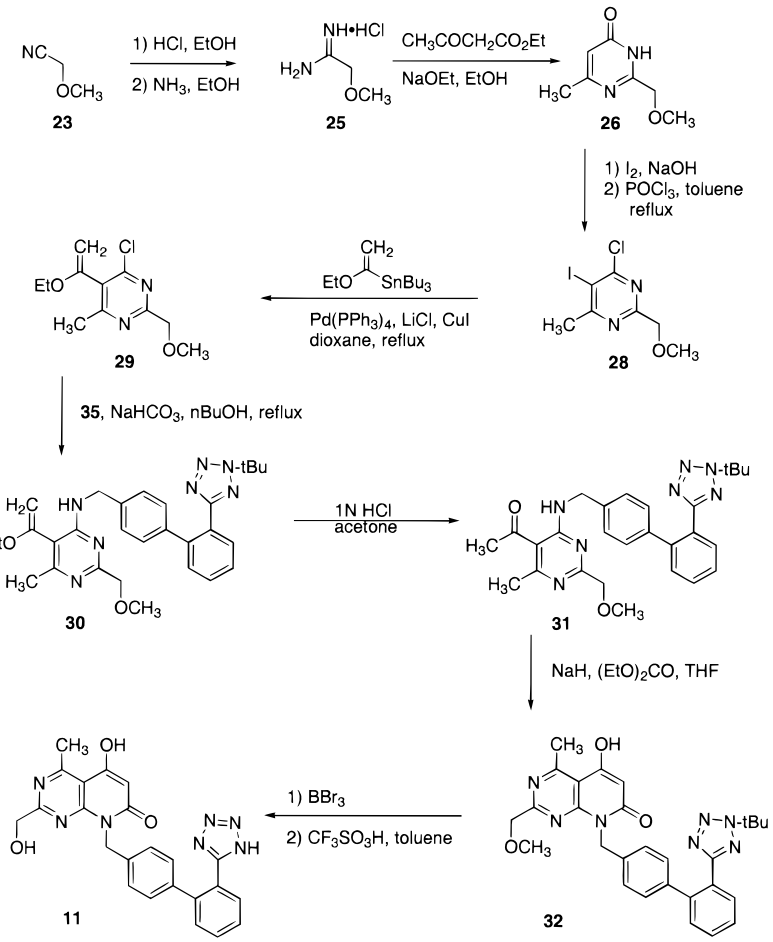

Scheme 5

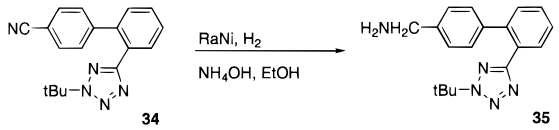

Scheme 6

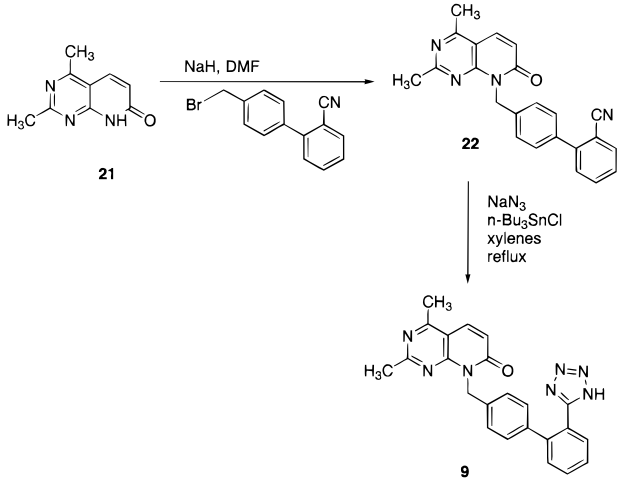

EXP3174 (**3**). A pharmacophore model based on these previous studies is illustrated in Figure 4, utilizing compound **8** as an example. Potential critical points of interaction with the AT_1 receptor are labeled 1−5. Also listed are the specific transmembrane domains and critical side chains based on the homology model.[14] The four minimal points of interaction[15] are labeled 1−4. Pharmacophore 1 is an acidic group, represented as a tetrazole in Figure 4, which is proposed to interact with Lys 199 in the homology model. Pharmacophore 2 represents a spacer (biphenyl group) which acts as a scaffold to properly orient the other pharmacophores. Pharmacophore 3 is an alkyl group that fits into a lipophilic pocket in the AT_1 receptor. In compounds **1** and **8** the lipophilic group is a methyl group whereas in **2** and **3** it is a butyl chain. Pharmacophore 4 is an aromatic nitrogen acting as a H-bond acceptor. The increased potency of metabolites **8** and **11**, and of the losartan metabolite **3**, relative to the parent drugs suggests that a fifth interaction is also important. Pharmacophore 5 is an acidic group which is proposed to interact with a basic side chain found on a surface loop of the AT_1 receptor.

Table 1. In Vitro Data for Metabolites

compd	IC_{50}, nM (n)[a]
1	1.20 ± 0.6 (3)
7	2.30 ± 1.6 (2)
8	0.17 ± 0.06 (3)
9	6.50 ± 0.26 (3)[b]
10	3.5% inhibition at 100 nM[b]
11	0.41 ± 0.10 (2)

[a] IC_{50} for inhibition of specific binding of [^{125}I]A II to rat adrenal membrane, mean ± SE, n = number of experiments. Each experiment represents an average of triplicate measurements. [b] IC_{50} for inhibition of specific binding of [^{125}I]A II to rat liver membrane.

The key structural difference between compounds **1**

Table 2. Dose Response Data for Compounds 1, 7, and 8 in the Goldblatt Hypertensive Rat after Intragastric and Intravenous Dosing

compd (route)	dose (mg/kg)	max decrease MAP (mmHg)[a]	n[b]	vehicle (n)[c]
1 (ig)	0.1	6 ± 8	6	6 ± 7 (10)
	0.3	45 ± 11[e,f]	6	11 ± 5 (10)
	1.0	71 ± 14[e,f]	6	11 ± 5 (10)
	3.0	76 ± 8[e,f]	9	11 ± 4 (10)
	10.0	81 ± 8[e,f]	12	11 ± 5 (10)
	30.0	80 ± 11[e,f]	6	12 ± 3 (10)
1 (iv)	0.1	37 ± 9[e]	7	6 ± 8 (5)
	1.0	53 ± 10[e,f]	8	10 ± 8 (5)
	3.0	54 ± 16[e,f]	7	9 ± 8 (5)
7 (ig)	1.0	55 ± 15[f]	6	11 ± 4 (12)
	3.0	54 ± 10[e,f]	7	11 ± 4 (12)
	10.0	71 ± 11	6	*d*
7 (iv)	1.0	51 ± 13	7	*d*
	3.0	47 ± 15	6	10 ± 6 (8)
	10.0	41 ± 8[f]	3	2 ± 7 (8)
8 (ig)	3.0	39 ± 12	6	4 ± 6 (12)
	10.0	66 ± 12[f]	6	4 ± 6 (12)
8 (iv)	0.03	34 ± 5	6	8 ± 5 (8)
	0.10	67 ± 11[f,g]	6	8 ± 5 (8)

[a] Maximum decrease in mean arterial pressure in mmHg after intragastric or intravenous dosing in Goldblatt (2K-1C) hypertensive rats, mean ± SE. [b] n = number of rats. [c] Decrease in mean arterial pressure in mmHg after intragastric or intravenous dosing of vehicle in Goldblatt (2K-1C) hypertensive rats, mean ± SE (n = number of rats). [d] Mean arterial pressure for vehicle treated rats not recorded. [e] $p < 0.05$ versus baseline (time 0). [f] $p < 0.05$ versus vehicle control. [g] $p < 0.05$ versus 0.03 mg/kg group.

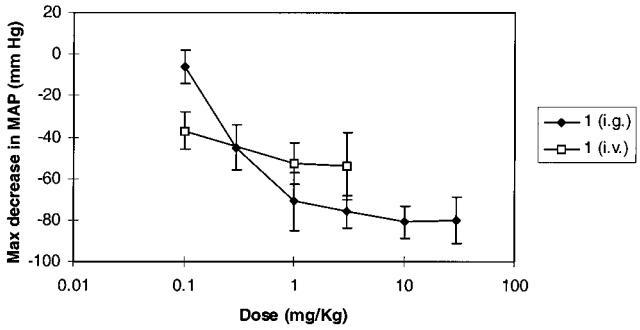

Figure 1. Change in MAP in Goldblatt hypertensive rats after ig and iv dosing of compound **1**.

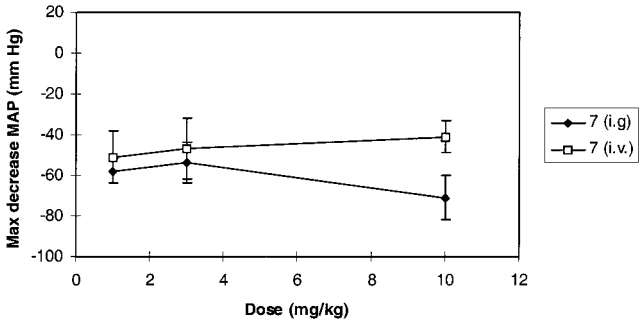

Figure 2. Change in MAP in Goldblatt hypertensive rats after ig and iv dosing of compound **7**.

and **8** as well as between **2** and **3** is the additional acidic group introduced metabolically. This group serves as pharmacophore 5 in the model and is in position to interact favorably with one of the basic side chains (Lys 102 or Arg 167) in the receptor surface loop.[14] This interaction may be responsible for the increase in potency seen with each pair of compounds. The pK_a of the enol in **8** is assumed to be about 9.7, which is less acidic than the carboxylic acid in **3**. However, an

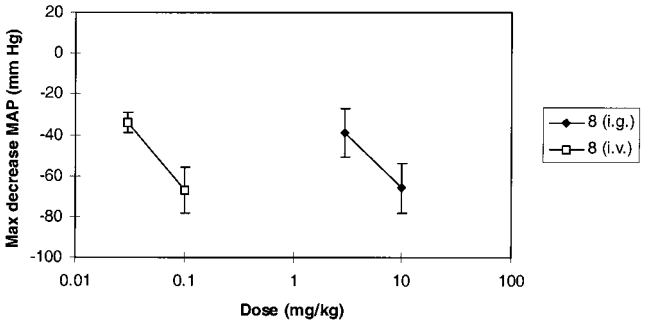

Figure 3. Change in MAP in Goldblatt hypertensive rats after ig and iv dosing of compound **8**.

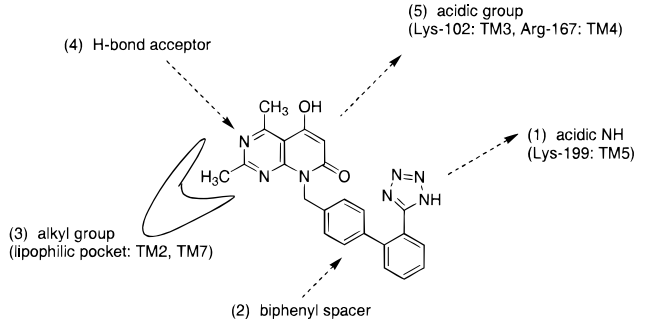

Figure 4. Proposed binding model for compound **8**.

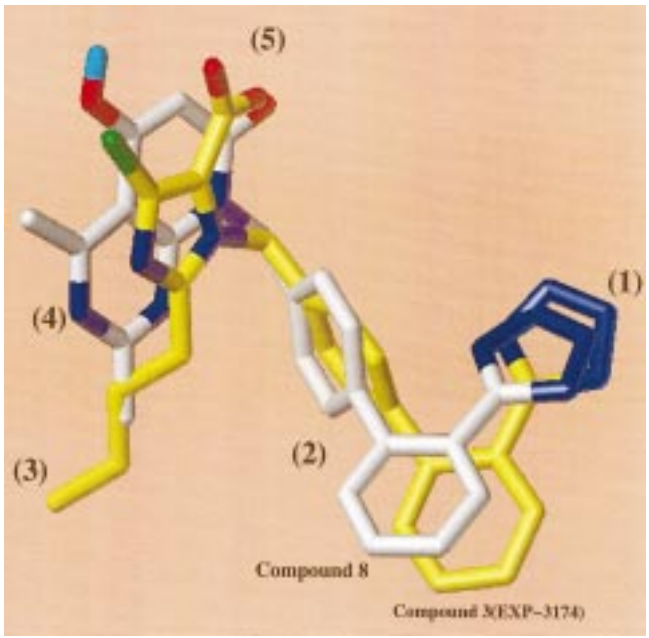

Figure 5. Overlap of compounds **3** and **8**.

interaction with a basic side chain should still be possible. Figure 5 illustrates the final superposition of compound **8** onto **3**, and the pharmacophores defined in Figure 4 are also indicated. The carboxylic acid of **3** and the enol of **8** occupy the same region so they could be interacting with the same basic residue. The isoelectric potential contour maps of compounds **1** and **8** and of **2** and **3** are shown in Figure 6. The isoelectric potential contours the electrostatic energy at 1 kcal/mol around each ligand. Red and blue represent the positive and negative electrostatic fields, respectively. It is evident that the metabolites **3** and **8** have enhanced negative electrostatic potentials around the region of pharmacophore 5. Thus, the carboxylic acid and enol

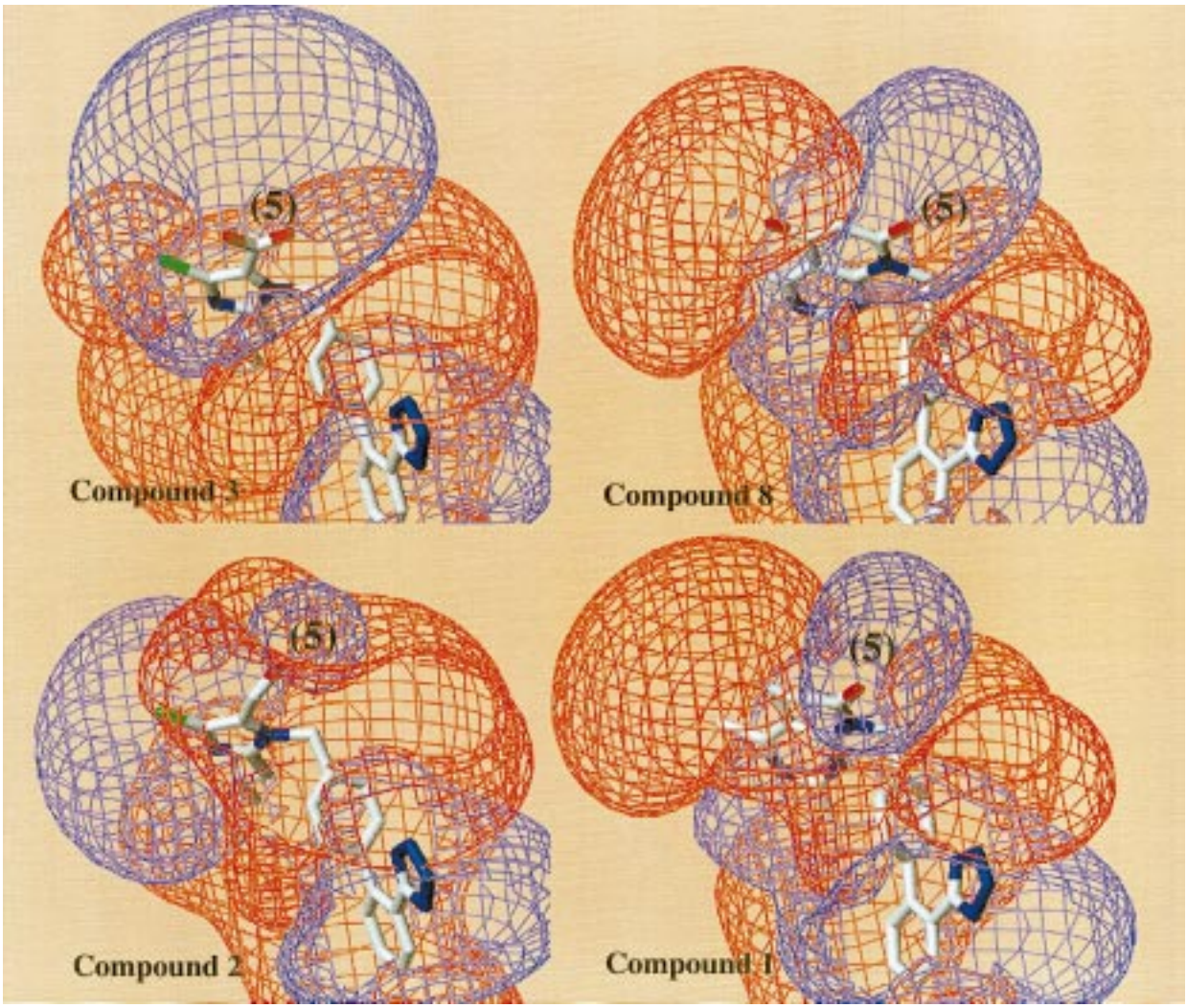

Figure 6. Isoelectric potential contour maps of compounds **1**, **2**, **3**, and **8**.

groups can display the same type of electrostatic character to a basic side chain in the receptor.

These modeling studies provide support for the idea that the enol group in compound **8** serves a role similar to that of the carboxylic acid group in compound **3** in contributing to the enhanced receptor binding shown by these compounds relative to their parent drugs.

Summary

Described in this paper is the synthesis and pharmacological activity of five metabolites of the A II antagonist tasosartan (**1**). The hydroxy metabolite **7** and the glucuronide **10** were synthesized directly from compound **1**. The remaining compounds required total syntheses to incorporate the different oxidation states of the pyrido ring. Of particular interest is the effect of the additional acidic group of the enol metabolites **8** and **11** on A II antagonist activity. Modeling studies suggest that the enol can interact with a basic side chain in the AT_1 receptor, and this additional interaction may enhance binding. Compound **8** is an order of magnitude more potent than **1** in the AT_1 receptor binding assay. However, **8** is an order of magnitude less potent than **1** in the Goldblatt hypertensive rat after oral dosing, probably because of poor absorption. The metabolic introduction of a second acidic group in **1** bypasses this problem and contributes to the excellent profile of the compound.

Experimental Section

Melting points were determined with a Thomas-Hoover apparatus and are uncorrected. The NMR spectra were recorded on a Varian VXR200, Varian VXR300, or a Bruker AM-400 instrument. The infrared spectra were recorded on a Perkin-Elmer diffraction grating or a Perkin-Elmer 784 spectrophotometer. The mass spectra were recorded on a Hewlett-Packard 5995A or a Finigan 8230 mass spectrometer. Analyses (C, H, N) were carried out on a modified Perkin-Elmer Model 240 CHN analyzer. Merck silica gel (70−230 mesh) was used for flash chromatography. Organic extracts were dried over $MgSO_4$ unless otherwise noted.

5-Hydroxy-2,4-dimethyl-8-[2′-(1*H*-tetrazol-5-yl)-biphenyl-4-ylmethyl]-6,8-dihydro-5*H*-pyrido[2,3-*d*]pyrimidine-7-one Sesquihydrate (7). To a cooled (0 °C), mechanically stirred mixture of **1**[11] (8.2 g, 0.020 mol), $MgSO_4$ (14.4 g, 0.120 mol), and water (285 mL) was added 2.5 N NaOH (8.78 mL). The resultant mixture was adjusted to pH 7.0−7.5 with 2 N HCl (0.7 mL). A solution of $KMnO_4$ (6.3 g, 0.040 mol) in water (362 mL) was added dropwise over 2 h 40 min, and the mixture was allowed to warm to room temperature. After 24 h, additional $MgSO_4$ (5.04 g, 0.042 mol) and $KMnO_4$ (2.2 g, 0.014 mol) were added, and stirring was continued for 24 h. The reaction mixture was filtered through Solka Floc, and the filtrate was concentrated to about 200 mL. The pH was adjusted to about 4 with KH_2PO_4 (13.6 g), and the precipitate was collected by filtration. The material was taken up in MeOH and filtered to give 1.96 g. The MnO_2 recovered by filtration through Solka Floc was stirred in water (400 mL) and filtered. The filtrate was treated with KH_2PO_4 to bring the pH to 4, and the precipitate was collected by filtration.

The material was taken up in methanol and filtered to give 1.36 g. The combined material was purified by flash chromatography (10−30% MeOH/$CHCl_3$), trituration with EtOAc and MeOH, and trituration with water to give 0.67 g (8%) of product as a white solid: mp 154−167 °C; ^{1}H NMR (DMSO-d_6) δ 2.44 (s, 3 H), 2.46 (s, 3 H), 2.79 (dd, J = 16.3, 2.4 Hz, 1 H), 2.99 (dd, J = 16.3, 4.0 Hz, 1 H), 4.97 (m, 1 H), 5.12 (d, J = 15.4 Hz, 1 H), 5.31 (d, J = 15.4 Hz, 1 H), 5.58 (d, J = 3.1 Hz, 1 H), 6.98 (d, J = 8.3 Hz, 2 H), 7.19 (d, J = 8.3 Hz, 2 H), 7.52 (m, 2 H), 7.63 (m, 2 H). Anal. ($C_{23}H_{21}N_7O_2 \cdot 1.5H_2O$) C, H, N.

2,4-Dimethyl-5-hydroxy-8-[2′-(1*H*-tetrazol-5-yl)biphenyl-4-ylmethyl]-8*H*-pyrido[2,3-d]pyrimidin-7-one (8). Step 1: 2,6-Dimethyl-5-iodo-4-hydroxypyrimidine (14). A mechanically stirred mixture of 2,6-dimethyl-4-hydroxypyrimidine (50.0 g, 0.403 mol), iodine (102.2 g, 0.403 mol), and 1 N NaOH (503 mL) was heated under reflux for 2 h. The mixture was extracted with $CHCl_3$ (some product fell out of solution and was collected by filtration: 24.5 g). The extracts were dried and concentrated to give 40.9 g of an orange solid which contained starting material and product. Trituration with EtOAc gave 26.0 g of product. The total yield of product was 50.5 g (50%): mp 208−210 °C (dec). An analytical sample was recrystallized from EtOH: mp 216−218 °C; ^{1}H NMR (DMSO-d_6) δ 2.21 (s, 3 H), 2.39 (s, 3 H), 12.58 (br s, 1 H). Anal. ($C_6H_7IN_2O$) C, H, N.

Step 2: 4-Chloro-2,6-dimethyl-5-iodopyrimidine (15). A mixture of **14** (24.5 g, 0.098 mol), phosphorus oxychloride (30.0 g, 0.196 mol), and toluene (200 mL) was heated under reflux for 1 h. The mixture was concentrated, and ice water (100 mL) was added. The pH was adjusted to 5 with 2.5 N NaOH and the mixture was extracted with CH_2Cl_2. The combined extracts were washed with brine, dried, and concentrated to give 24.6 g of a brown solid. The crude product was combined with 26.0 g of similarly prepared material and filtered through a short column of silica gel eluted with CH_2Cl_2 to give 33.8 g (62%) of product as a yellow solid. An analytical sample was recrystallized from hexane/CH_2Cl_2: mp 62−64 °C; ^{1}H NMR ($CDCl_3$) δ 2.61 (s, 3 H), 2.73 (s, 2 H). Anal. ($C_6H_6ClIN_2$) C, H, N.

Step 3: 4-Chloro-2,6-dimethyl-5-(1-ethoxyvinyl)pyrimidine (16). A mixture of **15** (13.5 g, 0.050 mol), (1-ethoxyvinyl)tributyltin (20.0 g, 0.055 mol), lithium chloride (6.4 g, 0.150 mol), tetrakis(triphenylphosphine)palladium(0) (1.7 g, 0.0015 mol), and dioxane (100 mL) was heated under reflux for 23 h. Additional tetrakis(triphenylphosphine)palladium(0) (1.1 g, 0.0010 mol) was added, and heating was continued for 25 h. The mixture was cooled and diluted with EtOAc, and 1 N KF (100 mL) was added. The solids were removed by filtration through Celite, and the layers were separated. The organic phase was washed with pH 7 phosphate buffer (100 mL) and brine (100 mL), dried, and concentrated. Purification by flash chromatography (twice; 5−10% EtOAc/hexane) gave 6.44 g (61%) of product as a colorless oil: ^{1}H NMR ($CDCl_3$) δ 1.35 (t, J = 7.0 Hz, 3 H), 2.49 (s, 3 H), 2.65 (s, 3 H), 3.91 (q, J = 7.0 Hz, 3 H), 4.21 (d, J = 2.8 Hz, 1 H), 4.52 (d, J = 2.8 Hz, 1 H). Anal. ($C_{10}H_{13}ClN_2O$) C, H, N.

Step 4: 4-(4-Bromobenzylamino)-2,6-dimethyl-5-(1-ethoxyvinyl)pyrimidine (17). A mixture of **16** (3.00 g, 0.0141 mol), 4-bromobenzylamine hydrochloride (3.45 g, 0.0155 mol), $NaHCO_3$ (2.37 g, 0.0282 mol), and *n*-BuOH (20 mL) was heated under reflux for 70 h. The mixture was concentrated, taken up in EtOAc, washed with water, dried, and concentrated. Trituration with ether/hexane gave 2.84 g (56%) of product as a white solid. An analytical sample was recrystallized from ether/hexane: mp 111−113 °C; ^{1}H NMR (DMSO-d_6) δ 1.24 (t, J = 6.9 Hz, 3 H), 2.15 (s, 3 H), 2.24 (s, 3 H), 3.84 (q, J = 6.9 Hz, 2 H), 4.18 (d, J = 1.7 Hz, 1 H), 4.50 (d, J = 6.2 Hz, 2 H), 4.53 (d, J = 1.7 Hz, 1 H), 6.91 (t, J = 6.2 Hz, 1 H), 7.22 (d, J = 8.3 Hz, 2 H), 7.46 (d, J = 8.3 Hz, 2 H). Anal. ($C_{17}H_{20}BrN_3O$) C, H, N.

Step 5: 2,6-Dimethyl-4-[*N*-(4-bromobenzylamino)]-5-acetylpyrimidine (18). A solution of **17** (2.72 g, 7.51 mmol), 1 N HCl (8.3 mL), and acetone (8 mL) was heated under reflux for 2.5 h. The acetone was removed under reduced pressure, and the aqueous phase was adjusted to pH 4 with 1 N KOH. The resultant white precipitate was collected by filtration to give 2.24 g (89%) of product as a white solid. An analytical sample was recrystallized from hexane: mp 78−80 °C; ^{1}H NMR (DMSO-d_6) δ 2.30 (s, 3 H), 2.36 (s, 3 H), 2.50 (s, 3 H), 4.57 (d, J = 5.8 Hz, 2 H), 7.25 (d, J = 8.3 Hz, 2 H), 7.49 (d, J = 8.3 Hz, 2 H), 8.34 (t, J = 5.8 Hz, 1 H). Anal. ($C_{15}H_{16}BrN_3O$) C, H, N.

Step 6: 2,6-Dimethyl-4-[*N*-(2′-(2-*tert*-butyl-2*H*-tetrazole-5-yl)-4-(methylamino)biphenyl)]-5-acetylpyrimidine (19). To a heated solution of **18** (1.67 g, 5.00 mmol) and tetrakis(triphenylphosphine)palladium(0) (0.29 g, 0.25 mmol) in toluene (20 mL) was added a partial solution of 2-[(2-*tert*-butyl)-2*H*-tetrazol-5-yl]phenylboronic acid[11] (1.50 g, 6.10 mmol) and Na_2CO_3 (1.06 g, 10.00 mmol) in water (10 mL) and EtOH (5 mL) in several portions over 1 h. Heating was continued for 2.5 h. The mixture was diluted with EtOAc, and the layers were separated. The organic phase was washed with 0.1 N NaOH and brine, dried, and concentrated. Purification by flash chromatography (40−50% EtOAc/hexane) and trituration with hexane gave 1.71 g (75%) of product as a white solid. An analytical sample was recrystallized from ether: mp 131−132 °C; ^{1}H NMR ($CDCl_3$) δ 1.54 (s, 9 H), 2.51 (s, 3 H), 2.56 (s, 3 H), 2.64 (s, 3 H), 4.71 (d, J = 5.7 Hz, 2 H), 7.12 (d, J = 8.3 Hz, 2 H), 7.22 (d, J = 8.3 Hz, 2 H), 7.45 (m, 3 H), 7.88 (m, 1 H), 9.0 (br s, 1 H). Anal. ($C_{26}H_{29}N_7O$) C, H, N.

Step 7: 2,4-Dimethyl-5-hydroxy-8-[2′-(2-*tert*-butyl-2*H*-tetrazol-5-yl)biphenyl-4-ylmethyl]-8*H*-pyrido[2,3-*d*]pyrimidin-7-one (20). To a heated suspension of NaH (60% dispersion in mineral oil; 0.24 g, 5.93 mmol) in diethyl carbonate (1.40 g, 11.85 mmol) and THF (10 mL) was added a solution of **19** (1.08 g, 2.37 mmol) in THF (10 mL) over 10 min. Heating was continued for 1.5 h. The mixture was concentrated, taken up in water, and extracted twice with ether (discarded). The aqueous phase was acidified to pH 4, and the precipitate was collected by filtration to give 965 mg (85%) of product. An analytical sample was recrystallized from acetone: mp 235−237 °C; ^{1}H NMR ($CDCl_3$) δ 1.47 (s, 9 H), 2.72 (s, 3 H), 2.89 (s, 3 H), 5.52 (s, 2 H), 6.18 (s, 1 H), 7.04 (d, J = 8.2 Hz, 2 H), 7.31 (d, J = 8.2 Hz, 2 H), 7.44 (m, 3 H), 7.84 (m, 1 H). Anal. ($C_{27}H_{27}N_7O_2$) C, H, N.

Step 8: 2,4-Dimethyl-5-hydroxy-8-[2′-(1*H*-tetrazol-5-yl)-biphenyl-4-ylmethyl]-8*H*-pyrido[2,3-*d*]pyrimidin-7-one Sesquihydrate (8). To a refluxing mixture of **20** (10 g, 0.020 mol) in toluene (250 mL) was added dropwise trifluoromethanesulfonic acid (10 mL). After 2 h, water (125 mL) was added dropwise and the mixture was cooled to room temperature. The toluene and water were decanted, and the residue was washed three times with water (decanted) and dried under a stream of N_2. The material was dissolved in THF and filtered through a pad of silica gel, eluting with 2.5% AcOH in THF. The mixture was concentrated, EtOAc was added, and the mixture was concentrated to give an oil. Water was added, and the mixture was concentrated (twice). After the second addition of water and concentration the compound crystallized. The material was filtered and washed with water to give 7.4 g (84%) of product. Recrystallization of 520 mg of similarily prepared product from EtOH/water gave 424 mg of product as an off-white solid: mp 278−280 °C (dec); ^{1}H NMR (DMSO-d_6) δ 2.55 (s, 3 H), 2.80 (s, 3 H), 5.43 (s, 2 H), 5.86 (s, 1 H), 6.99 (d, J = 8.1 Hz, 2 H), 7.14 (d, J = 8.1 Hz, 2 H), 7.42 (m, 1 H), 7.47 (dd, J = 7.7, 1.5 Hz, 1 H), 7.54 (m, 1 H), 7.58 (dd, J = 7.5, 1.5 Hz, 1 H). Anal. ($C_{23}H_{19}N_7O_2 \cdot 1.5H_2O$) C, H, N.

2,4-Dimethyl-8-[2′-(1*H*-tetrazol-5-yl)-biphenyl-4-ylmethyl]-8*H*-pyrido[2,3-*d*]pyrimidin-7-one (9). Step 1: 2,4-Dimethyl-8-[[2′-cyano[1,1-biphenyl]-4-yl]methyl]-7*H*-pyrido[2,3-*d*]pyrimidin7-one (22). To a suspension of NaH (60% dispersion in mineral oil; 0.123 g, 3.08 mmol) in DMF (10 mL) was added 2,4-dimethyl-7*H*-pyrido[2,3-*d*]pyrimidin-7-one (**21**) (0.54 g, 3.08 mmol), prepared according to Sakamoto et al.[13] The reaction mixture was stirred at room temperature for 1 h, and 2-[4-(bromomethyl)phenyl]benzonitrile (1.00 g, 3.7 mmol) was added. Stirring was continued for 5 h, and the

mixture was concentrated and taken up in water. The aqueous layer was extracted with CH_2Cl_2, and the combined extracts were dried and concentrated. Purification by flash chromatography (2% MeOH/CH_2Cl_2) and trituration with ether gave 0.65 g (58%) of product as a yellow solid: mp 177−179 °C; ^{1}H NMR (DMSO-d_6) δ 2.63 (s, 3 H), 2.69 (s, 3 H), 5.61 (s, 2 H), 6.72 (d, J = 9.6 Hz, 1 H), 7.50 (m, 6 H), 7.76 (m, 1 H), 7.91 (d, J = 7.6 Hz, 1 H), 8.20 (d, J = 9.6 Hz, 1 H).

Step 2: 2,4-Dimethyl-8-[2′-(1*H*-tetrazol-5-yl)-biphenyl-4-ylmethyl]-8*H*-pyrido[2,3-*d*]pyrimidin-7-one (9). A mixture of **22** (0.65 g, 1.8 mmol), *n*-Bu_3SnCl (0.75 g, 2.3 mmol), NaN_3 (0.15 g, 2.3 mmol), and xylene (8.0 mL) was heated under reflux for 48 h. The reaction mixture was cooled, and 1 N HCl was added. The mixture was extracted with EtOAc, and the layers were separated. The organic phase was extracted with 1 N NaOH, and the combined basic layers were acidified to pH 4 and extracted with CH_2Cl_2. The combined extracts were dried and concentrated to give a yellow oil. The oil was triturated and recrystallized from EtOH to give 0.26 g (55%) of product as an off-white solid: mp 253−255 °C; ^{1}H NMR (DMSO-d_6) δ 2.60 (s, 3 H), 2.68 (s, 3 H), 5.51 (s, 2 H), 6.71 (d, J = 9.6 Hz, 1 H), 7.00 (d, J = 8.0 Hz, 2 H), 7.20 (d, J = 8.0 Hz, 2 H), 7.59 (m, 4 H), 8.20 (d, J = 9.6 Hz, 1 H). Anal. ($C_{23}H_{19}N_7O$) C, H. N: calcd, 23.95; found, 23.42.

1-Deoxy-1-{5-[4′-(7-oxo-6,7-dihydro-5*H*-pyrido[2,3-*d*]-pyrimidin-8-ylmethyl)-biphenyl-2-yl]-tetrazol-2-yl}-*β*-D-glucuronic Acid Sodium Salt Monohydrate (10). Step 1: 1-Deoxy-2,3,4-tri-*O*-acetyl-1-{5-[4′-(7-oxo-6,7-dihydro-5*H*-pyrido[2,3-*d*]pyrimidin-8-ylmethyl)-biphenyl-2-yl]-tetrazol-2-yl}-*β*-D-glucuronic Acid Methyl Ester (12a). To a solution of **1** (1.27 g, 3.1 mmol) in MeOH (10 mL) was added 1 N KOH (3.1 mL). The mixture was concentrated, and the potassium salt was dissolved in acetone (14 mL). Bromo-2,3,4-tri-*O*-acetyl-α-D-glucopyranuronic acid methyl ester (1.4 g, 3.55 mmol) was added, and the mixture was heated under reflux for 18 h. The mixture was cooled, concentrated, and purified by flash chromatography (20% acetone/Et_2O) to give 0.77 g (34%) of N-2 glucuronide product (**12a**) and 0.40 g (18%) of N-1 glucuronide product (**12b**). **12a**: ^{1}H NMR ($CDCl_3$) δ 2.04 (s, 3 H), 2.05 (s, 3 H), 2.40 (s, 3 H), 2.57 (s, 3 H), 2.73 (t, J = 6.5 Hz, 2 H), 2.84 (t, J = 6.9 Hz, 2 H), 3.74 (s, 3 H), 4.28 (d, J = 9.5 Hz, 1 H), 5.29 (s, 2 H), 5.40 (m, 2 H), 5.80 (t, J = 9.3 Hz, 1 H), 6.02 (d, J = 9.3 Hz, 1 H), 7.04 (d, J = 6.5 Hz, 1 H), 7.50 (m, 5 H), 7.78 (dd, J = 7.3, 1.5 Hz, 1 H). **12b**: ^{1}H NMR ($CDCl_3$) δ 1.71 (s, 3 H), 1.98 (s, 3 H), 1.99 (s, 3 H), 2.40 (s, 3 H), 2.56 (s, 3 H), 2.70 (t, J = 7.9 Hz, 2 H), 2.84 (t, J = 8.0 Hz, 2 H), 3.75 (s, 3 H), 3.77 (d, J = 7.5 Hz, 1 H), 5.20 (m, 5 H), 5.66 (t, J = 8.9 Hz, 1 H), 7.04 (d, J = 8.3 Hz, 2 H), 7.35 (d, J = 8.3 Hz, 1 H), 7.55 (m, 3 H), 7.65 (m, 1 H).

Step 2: 1-Deoxy-1-{5-[4′-(7-oxo-6,7-dihydro-5*H*-pyrido-[2,3-*d*]pyrimidin-8-ylmethyl)-biphenyl-2-yl]-tetrazol-2-yl}-*β*-D-glucuronic Acid Methyl Ester (13). To a solution of **12a** (1.1 g, 1.50 mmol) in MeOH (30 mL) was added KCN (50 mg, 0.75 mmol), and the mixture was stirred at room temperature for 5 h. The mixture was concentrated and purified by flash chromatography (5% MeOH/CH_2Cl_2) to give 0.57 g (63%) of product as a white foam: ^{1}H NMR (DMSO-d_6) δ 2.36 (s, 3 H), 2.44 (s, 3 H), 2.72 (t, J = 7.9 Hz, 2 H), 2.88 (t, J = 7.7 Hz, 2 H), 3.51 (m, 2 H), 3.68 (s, 3 H), 3.94 (m, 1 H), 4.26 (d, J = 9.1 Hz, 1 H), 5.19 (s, 2 H), 5.47 (d, J = 5.2 Hz, 1 H), 5.60 (d, J = 5.2 Hz, 1 H), 5.66 (d, J = 5.5 Hz, 1 H), 6.04 (d, J = 9.2 Hz, 1 H), 7.03 (d, J = 8.0 Hz, 2 H), 7.18 (d, J = 8.1 Hz, 2 H), 7.55 (m, 2 H), 7.76 (d, J = 7.5 Hz, 1 Hz).

Step 3: 1-Deoxy-1-{5-[4′-(7-oxo-6,7-dihydro-5*H*-pyrido-[2,3-*d*]pyrimidin-8-ylmethyl)-biphenyl-2-yl]-tetrazol-2-yl}-*β*-D-glucuronic Acid Sodium Salt Monohydrate (10). To a solution of (**13**) (0.53 g, 0.89 mmol) in MeOH (5 mL) was added 1 N NaOH (0.89 mL), and the mixture was stirred at room temperature for 3 h. The mixture was filtered to give 0.35 g (62%) of a white solid: mp 226−228 °C (dec); ^{1}H NMR (DMSO-d_6) δ 2.36 (s, 3 H), 2.45 (s, 3 H), 2.72 (t, J = 8.3 Hz, 2 H), 2.88 (t, J = 7.5 Hz, 2 H), 3.23 (m, 1 H), 3.37 (m, 1 H), 3.56 (d, J = 10.0 Hz, 1 H), 3.83 (m, 1 H), 5.18 (d, J = 5.0 Hz, 1 H), 5.19 (s, 2 H), 5.40 (d, J = 5.8 Hz, 1 H), 5.72 (d, J = 9.1 Hz, 1 H), 7.05 (d, J = 8.3 Hz, 2 H), 7.19 (d, J = 8.3 Hz, 2 H), 7.38 (br s, 1 H), 7.55 (m, 3 H), 7.78 (dd, J = 7.5, 1.2 Hz, 1 Hz). Anal. ($C_{29}H_{28}N_7NaO_7 \cdot H_2O$) H, N. C: calcd, 55.45; found, 54.90.

5-Hydroxy-2-hydroxymethyl-4-methyl-8-[2′-(1*H*-tetrazol-5-yl)-biphenyl-4-ylmethyl]-8*H*-pyrido[2,3-*d*]pyrimidin-7-one (11). Step 1: 2-Ethoxy-3-methoxy Imidate Hydrochloride (24). To a solution of methoxyacetonitrile (120 g, 1.6882 mol) in EtOH (99 mL) and Et_2O (500 mL) at −15 °C (ice/MeOH bath) was added HCl gas rapidly for 20 min, until the solution was at or near saturation. This solution was stirred overnight at room temperature under a nitrogen atmosphere. The mixture was recooled to −15 °C, and the solid was vacuum-filtered, washed with ether, and dried by drawing dry nitrogen gas through the solid for 1 h using a vacuum filtration apparatus. The yield of white solid was 216.1 g (83.3%): ^{1}H NMR (300 MHz, DMSO-d_6) δ 1.38 (t, J = 7.0 Hz, 3 H), 3.42 (s, 3 H), 4.42 (s, 2 H), 4.54 (q, J = 7.0 Hz, 2 H).

Step 2: **1-Methoxyacetamidine Hydrochloride (25).** Dry EtOH (1.0 L) was cooled to −15 °C, and anhydrous ammonia (65.0 g) was added followed by **24** (200.0 g, 1.302 mol); a small amount of EtOH was used to wash in any remaining solid. This mixture was stirred at room temperature overnight. It was recooled to −15 °C, and a small amount of solid was filtered. The filtrate was placed on an evaporator to remove the solvent and then under high vacuum to remove the last traces of solvent. The clear oil spontaneously crystallized to give 162.2 g of a white solid (100%): ^{1}H NMR (300 MHz, DMSO-d_6) δ 3.39 (s, 3 H), 4.26 (s, 2 H), 9.00 (br s).

Step 3: **2-Methoxymethyl-6-methyl-4-pyrimidone (26).** To a solution of NaOEt/EtOH, made from EtOH (1419 mL) and sodium (55.4 g), was added **25** (150.0 g, 1.204 mol) and ethylacetoacetate (156.71 g, 1.204 mol). This mixture was heated to reflux for 18 h. The reaction mixture was cooled, and the EtOH was removed on a rotary evaporator. The solids were dissolved in water, and the pH was adjusted to 5.5 using concentrated HCl. The aqueous mixture was extracted with CH_2Cl_2 and ethyl acetate. The organics were combined, washed with brine, dried (Na_2SO_4), filtered and evaporated to leave a light-yellow solid. The solid was triturated using EtOAc/hexane (2/3), collected via vacuum filtration, and placed under high vacuum for 3 h. The yield of white solid was 126.0 g (68%): ^{1}H NMR (300 MHz, DMSO-d_6) δ 2.15 (s, 3 H), 3.31 (s, 3 H), 4.21 (s, 2 H), 6.08 (s, 1 H); IR (KBr), cm^{-1} 1680 (s), 910 (vs); MS (EI) M^+ m/z 154, $(M - OCH_3)^+$ m/z 124.

Step 4: 2-Methoxymethyl-5-iodo-6-methyl-4-pyrimidone (27). To a well-stirred solution of **26** (15.0 g, 0.0973 mol) in 1.25 N NaOH (160 mL) was added iodine (25.4 g, 0.10 mol). When the iodine was in solution the mixture was heated to reflux (110 °C oil bath) for 2 h. The solution was then cooled to 0 °C and held there for 1 h. During this time, a solid precipitated and it was collected via vacuum filtration and washed with a little cold water. The filtrate was extracted with $CHCl_3$, dried (Na_2SO_4), filtered, and evaporated to leave a solid that was a mixture of starting material and product. Flash chromatography (silica gel, EtOAc as eluant) was used to separate these components and afford 10.5 g of pure product (both crystalline precipitate and chromatographed material). The yield was 52.5% (corrected for 4.0 g of starting material recovered): ^{1}H NMR (300 MHz, $CDCl_3$) δ 2.57 (s, 3 H), 3.54 (s, 3 H), 4.38 (s, 2 H), 10.70 (br s, 1 H); IR (KBr), cm^{-1} 1645 (vs), 1000 (s); MS (EI) M^+ m/z 280, $(m - OCH_3)^+$ m/z 250.

Step 5: **2-Methoxymethyl-4-chloro-5-iodo-6-methylpyrimidine (28).** To a well-stirred solution of **27** (50.0 g, 0.1785 mol) in toluene at room temperature was added phosphorus oxychloride (2 equiv, 34.2 mL). The mixture was heated to reflux (115 °C oil bath) for 1.5 h, then cooled to approximately 10 °C, and quenched with ice water. The toluene was removed on an evaporator, and 150 mL of cold water were added. The pH was adjusted to 5.5 with 2.5 N aqueous NaOH, and the mixture was extracted with CH_2Cl_2. The combined extracts were washed with brine, dried (Na_2SO_4), filtered, and evaporated. Final purification by flash chromatography (short silica column, CH_2Cl_2/EtOAc as eluant) afforded 48.5 g (91%) of the

product as a light tan oil: ^{1}H NMR (300 MHz, $CDCl_3$) δ 2.82 (s, 3 H), 3.53 (s, 3 H), 4.59 (s, 2 H).

Step 6: 2-Methoxymethyl-4-chloro-5-(1-ethoxyvinyl)-6-methylpyrimidine (29). A mixture of **28** (39.80 g, 0.1333 mol), (1-ethoxyvinyl)tributyltin (48.15 g, 0.1333 mol), lithium chloride (19.5 g, 0.46 mol), and copper(I) iodide (1.0 g) in dry dioxane (250 mL) was deoxygenated for 20 min using a stream nitrogen gas. To this mixture was then added tetrakis-(triphenylphosphine)palladium(0) (8.1 g, 0.007 mol) and tris-(dibenzylideneacetone)dipalladium(0) (3.0 g, 0.0033 mol), and it was heated to mild reflux (105 °C oil bath) for 40 h. The mixture was cooled, diluted with EtOAc (250 mL), and treated with 1 N aqueous KF (200 mL). This was stirred for 20 min and then filtered through Celite. The layers were separated, the aqueous phase was extracted with EtOAc, the organics were combined, washed with brine, dried (Na_2SO_4), filtered, and evaporated. The product was purified by flash chromatography (silica gel, EtOAc/hexane (9/1) as eluant) to afford 24.3 g (75%) of product as a light-yellow oil: ^{1}H NMR (300 MHz, $CDCl_3$) δ 1.38 (t, J = 7.0 Hz, 3 H), 2.58 (s, 3 H), 3.53 (s, 3 H), 3.94 (t, J = 7.0 Hz, 2 H), 4.25 (d, J = 2.9 Hz, 1 H), 4.55 (d, J = 2.9 Hz, 1 H), 4.62 (s, 2 H).

Step 7: 2′-(2-*tert*-Butyl-2*H*-tetrazole-5-yl)-4-methylaminobiphenyl (35). A mixture of 2′-(2-*tert*-butyl-2*H*-tetrazole-5-yl)-4-cyanobiphenyl (**34**) (30.70 g, 0.1012 mol), Raney nickel (9.0 g), concentrated ammonium hydroxide (90 mL), and EtOH (425 mL) was placed into a 1 L vessel under 50 psig of hydrogen gas on a Parr apparatus. The vessel was shaken for 22 h while maintaining a pressure of 50 psig. The mixture was then filtered through Celite and evaporated. The residue was dissolved in CH_2Cl_2, washed with brine, dried (Na_2SO_4), filtered, and evaporated to leave a colorless oil. High vacuum for 4 h afforded 31.1 g (100%) of pure product that was used as is in the next step: ^{1}H NMR (300 MHz, $CDCl_3$) δ 1.60 (s, 9 H), 3.86 (s, 2 H), 7.14−7.90 (series of m, 8 H).

Step 8: 2-Methoxymethyl-4-[*N*-(2′-(2-*tert*-butyl-2*H*-tetrazole-5-yl)-4-(methylamino)biphenyl)]-5-(1-ethoxyvinyl)-6-methylpyrimidine (30). A mixture of **35** (28.28 g, 0.092 mol), **29** (20.30 g, 0.0836 mol), and $NaHCO_3$ (7.73 g, 0.092 mol) in *n*-butyl alcohol (105 mL) was heated to 120 °C for 48 h. The cooled mixture was evaporated in vacuo, and the residue was dissolved in EtOAc and washed with dilute brine (2×). The organic phase was dried (Na_2SO_4), filtered, evaporated, and placed under high vacuum. The product was used as is in the next step. The yield was 42.0 g (98%) of unpurified material: ^{1}H NMR (300 MHz, $CDCl_3$) δ 1.33 (t, J = 7.0 Hz, 3 H), 1.56 (s, 9 H), 2.38 (s, 3 H), 3.50 (s, 3 H), 3.87 (q, J = 7.0 Hz, 2 H), 4.27 (d, J = 2.2 Hz, 1 H), 4.46 (s, 2 H), 4.53 (d, J = 2.2 Hz, 1 H), 4.68 (d, J = 5.6 Hz, 2 H), 5.59 (m, 1 H), 7.15−7.87 (series of m, 8 H).

Step 9: 2-Methoxymethyl-4-[*N*-(2′-(2-*tert*-butyl-2*H*-tetrazole-5-yl)-4-(methylamino)biphenyl)]-5-acetyl-6-methylpyrimidine (31). To a solution of **30** (41.5 g, 0.0808 mol) in acetone (125 mL) was added 1 N aqueous HCl (125 mL). This mixture was heated to reflux (65 °C oil bath) for 2.5 h. The mixture was then cooled, the acetone evaporated, the pH adjusted to 5.0, and the mixture extracted with CH_2Cl_2. The combined extracts were dried (Na_2SO_4), filtered, and evaporated. The product was purified by flash chromatography (silica gel; Et_2O/EtOAc first 3/1, then 1/1 as eluant) to afford 30.1 g (74%, two steps) of a yellow oil: ^{1}H NMR (300 MHz, $CDCl_3$) δ 1.56 (s, 9 H), 2.58 (s, 3 H), 2.68 (s, 3 H), 3.52 (s, 3 H), 4.47 (s, 2 H), 4.73 (d, J = 5.6 Hz, 2 H), 7.15−7.90 (series of m, 8 H), 8.86 (br m, 1 H); MS (+FAB), $[M + H]^+$ m/z 486.

Step 10: 2-Methoxymethyl-5-hydroxy-8-[*N*-(2′-(2-*tert*-butyl-2*H*-tetrazole-5-yl)-4-yl-methylbiphenyl)]-8*H*-pyrido-[2,3-*d*]pyrimidine-7-one (32). To a heated suspension (60 °C oil bath) of NaH (60% in oil, 1.51 g, 0.0377 mol) and diethyl carbonate (9.14 mL, 0.0754 mol) in THF (65 mL) was added, over 20−30 min, a solution of **31** in THF (40 mL). After the addition, the solution was heated to reflux for 2 h. The cooled mixture (10 °C) was quenched with water (5 mL), and pH 4 buffer was added until the pH of the reaction mixture was 5.0. The THF was removed on an evaporator, and the aqueous phase was filtered. The aqueous filtrate was extracted with CH_2Cl_2 and EtOAc; the filtered solid was treated with EtOAc/MeOH (3/1, 160 mL) and filtered, and the filtrate was combined with the other organic extracts. The organic solution was dried (Na_2SO_4), filtered, and evaporated. The product was purified by flash chromatography (silica gel; CH_2Cl_2/MeOH, 25/1, as eluant) to give 5.575 g (72%) of a white solid. Four identical experiments of the above were run to give 22.3 g of product: ^{1}H NMR (400 MHz, DMSO-d_6) δ 1.36 (s, 9 H), 2.84 (s, 3 H), 3.32 (s, 3 H), 4.52 (s, 2 H), 5.46 (s, 2 H), 5.91 (s, 1 H), 6.96 (d, J = 8.35 Hz, 2 H), 7.25 (d, J = 8.35 Hz, 2 H), 7.42 (m, 1 H), 7.51(m, 1 H), 7.58 (m, 1 H), 7.74 (m, 1 H), 11.98 (br, 1 H); ^{1}H NMR (400 MHz, $CDCl_3$) δ 1.49 (s, 9 H), 2.91 (s, 3 H), 3.52 (s, 3 H), 4.67 (s, 2 H), 5.58 (s, 2 H), 6.21 (s, 1 H), 7.04 (d, J = 8.35 Hz, 2 H), 7.33 (s, 1 H), 7.36 (d, J = 8.35 Hz, 2 H), 7.45 (m, 2 H), 7.83 (m, 1 H), 11.60 (br s, 1 H); MS (EI) M^+ m/z 511.

Step 11: 2-Hydroxymethyl-5-hydroxy-8-[*N*-(2′-(2-*tert*-butyl-2*H*-tetrazole-5-yl)-4-yl-methylbiphenyl)]-8*H*-pyrido-[2,3-*d*]pyrimidine-7-one (33). To a well-stirred solution of **32** (11.4 g, 0.0223 mol) in CH_2Cl_2 (100 mL) at 0 °C was added BBr_3 (55.75 mL of a 1 M solution in CH_2Cl_2). A solid formed immediately. The reaction mixture was warmed slowly to 45 °C and held there for 2.5 h. TLC indicated the absence of starting material. The reaction mixture was cooled to 0 °C, and 1.25 N aqueous NaOH (175 mL) was added rapidly dropwise. This was stirred for 2 h at 0 °C and allowed to come to room temperature. The pH was adjusted to 6.0, the layers were separated, and the aqueous layer was extracted with CH_2Cl_2. The combined organic extracts were dried (Na_2SO_4), filtered, and evaporated. The product was purified by flash chromatography (silica gel; CH_2Cl_2/MeOH, 20/1, as eluant) to afford 8.05 g (72.5%) of white solid. Another smaller scale experiment was run for an additional 6.85 g: ^{1}H NMR (300 MHz, $CDCl_3$) δ 1.51 (s, 9 H), 2.83 (s, 3 H), 3.74 (br s, 1 H), 4.81 (s, 2 H), 5.51 (s, 2 H), 6.13 (s, 1 H), 7.06 (d, J = 8.35 Hz, 2 H), 7.27 (d, J = 8.35 Hz, 2 H), 7.33 (m, 1 H), 7.45 (m, 2 H), 7.84 (m, 1 H), 12.20 (br s, 1 H); ^{1}H NMR (400 MHz, DMSO-d_6) δ 1.37 (s, 9 H), 2.88 (s, 3 H), 4.49 (s, 2 H), 5.12 (br s, 1 H), 5.45 (s, 2 H), 5.47 (s, 1 H), 6.93 (d, J = 8.13 Hz, 2 H), 7.10 (br, 1 H), 7.27 (d, J = 8.13 Hz, 2 H), 7.43 (m, 1 H), 7.50 (m, 1 H), 7.56 (m, 1 H), 7.75 (m, 1 H); MS (EI), M^+ m/z 497.

Step 12: 2-Hydroxymethyl-5-hydroxy-8-[*N*-(2′-(2*H*-tetrazole-5-yl)-4-yl-methylbiphenyl)]-8*H*-pyrido[2,3-*d*]pyrimidine-7-one (11). A mixture of **33** (0.005 g, 0.01 mmol), toluene (0.25 mL), and trifluoromethanesulfonic acid (0.01 mL), under nitrogen atmosphere, was heated in an oil bath at 115 °C for 2 h. The mixture was cooled to approximately 20 °C, methanol (1 mL) and water (0.5 mL) were added, and the pH was adjusted to 5.5. The organic solvents were removed on an evaporator, and an aqueous suspension resulted. The solids were collected by vacuum filtration, washed with water, then with ethyl acetate/ether (1/1), and sucked dry in a small fine sintered glass funnel under a flow of nitrogen gas for 1 h. The solid was purified by prep-layer chromatography using silica gel, and the eluant was dichloromethane/methanol/acetic acid (91/9.5/0.5). The material was placed under high vacuum at 70 °C for 22 h to yield 0.003 g (67%) of a white solid: ^{1}H NMR (400 MHz, DMSO-d_6) δ 2.83 (s, 3 H), 4.55 (s, 2 H), 5.10 (br, 1 H), 5.50 (s, 2 H), 5.89 (s, 1 H), 6.97 (d, J = 8.35 Hz, 2 H), 7.25 (d, J = 8.35 Hz, 2 H), 7.51 (m, 2 H), 7.62 (m, 2 H), 11.97 (s, 1 H); MS (+FAB), $[M + H]^+$ m/z 442. A second batch of 11.8 g was prepared in a similar fashion. HPLC (inertsil, 5/95−80/20 CH_3CN/10 mM KH_2PO_4, pH = 3.50) showed the compound to be 99.92% pure. Anal. ($C_{23}H_{19}N_7O_3 \cdot 1.5H_2O$) H, N. H: calcd, 4.73; found, 4.14.

pK_a Determination. The pK_a values for compound **20** were determined by potentiometric titration with a Sirius GLpK_a titrator. A sample of **20** (2−5 mg) was dissolved in 0.15 M KCl with 15−57% methanol and titrated with 0.5 M HCl from pH 1.8 to pH 11.5. All of the samples were sonicated at pH 1.8 before titration to ensure complete dissolution. No precipitation appeared during the titration at this pH range as monitored by a turbidity probe. The aqueous pK_a values

were obtained from extrapolation of the five apparent pK_a values in the presence of methanol to 0% methanol. Three pK_a values were obtained for **20** at 0% methanol: 9.73 ± 0.37, 6.20 ± 0.17, and 2.48 ± 0.18. The slope of the linear plot of the apparent pK_a values in the presence of methanol as a function of the solvent dielectric constant is positive for the value of 9.73, which indicates that the pK_a value is due to an acidic group. The negative slopes for the values of 6.20 and 2.48 are a result of ionization from basic groups.

Molecular Modeling. Molecular models were generated using Sybyl (v6.4) molecular modeling software from Tripos Associates.[16] The conformations of the ligand models used in this study were set as close as possible to the conformations found in recent studies[14,15] based on stereo diagrams and specific distance constraints. Each model was minimized to its local minimum using MAXIMIN2.[16] Solvent conditions were represented implicitly using a distance-dependent dielectric constant along with a nonbonded cutoff set to 15 Å; atom partial charges were generated using the semiempirical method MOPAC.[16] All ligands were superimposed for comparison using a rigid body fitting algorithm called FIT[16] where specific pharmacophore atoms represented in all of the ligands were superimposed.

Pharmacology: [^{125}I]A II Binding Assay. Rat liver membrane was obtained as a kit from New England Nuclear (NED-014A, Boston, MA). The membrane was diluted and the A II reconstituted with the diluent buffer provided with the kit. The final concentrations of A II were 10^{-10} to 10^{-7} M for the standard and 10^{-4} M for determination of the nonspecific binding. The [^{125}I]A II was diluted in deionized water. The test compounds were dissolved in 50% DMSO as concentrates. For the assay, 25 μL of a standard, reference, test compound or vehicle was pipetted into appropriate test tubes. In addition, 25 μL of diluted [^{125}I]A II and 200 μL of membrane suspension were pipetted into each test tube. The contents of the test tube were mixed and incubated for 3 h at room temperature. The incubation was stopped by addition of saline and filtration on to a glass fiber filter. The filter disks were counted in a gamma counter to determine the [^{125}I]A II binding to the rat liver membrane. The IC_{50} values were determined as the concentration of the compound required to inhibit the specific [^{125}I]A II binding by 50% of the vehicle control.

Goldblatt (2K-1C) Hypertensive Rats. Sprague−Dawley rats weighing 150 g were anesthetized with pentobarbital (50 mg/kg ip), and the left renal artery was clipped with a silver wire bent to an internal diameter of 0.2 mm. The hypertension was established 4−7 weeks after clipping. At that time, the animals were anesthetized with pentobarbital (50 mg/kg ip), and the right carotid artery was cannulated. The catheter was passed subcutaneously to the dorsal side of the neck and exteriorized. The animals were fasted overnight but allowed access to water, and the experiment was performed the next morning. The carotid catheter was connected to a blood pressure transducer which was linked to a MI^2 computer data acquisition system or to a Grass or Beckman recorder for the recording of mean arterial pressure and heart rate. The rats were given either compound **1**, **7**, **8**, or vehicle (0.5% methyl cellulose in distilled water) by gastric gavage in a volume of 5 mL/kg. In the experiments with **1**, **7**, and **8**, saline was infused into the arterial cannula at 5 μL/min throughout the experiment to maintain patency of the cannula. A separate vehicle control group was run with a saline infusion into the arterial cannula. Each compound was administered to a separate group of 6−12 rats and MAP and heart rate were recorded for 24 h. Data were recorded every 15 min for the first hour, every 30 min for the second hour, hourly up to 8 h, and then at 22, 23, and 24 h following dosing. At each time point following dosing, averages were determined for absolute MAP, change in MAP (in mmHg), and heart rate for all animals, and the standard error of the mean was calculated.

Acknowledgment. We express our appreciation to the Analytical Department of Wyeth-Ayerst for elemental analyses and spectral data.

References

(1) Ferrarro, C. M. The Renin-Angiotensis System: Importance in Physiology and Pathology. *J. Cardiovasc. Pharmacol.* **1990**, *15* (Suppl. 3), S1−S5.
(2) McAreavey, D. Robertson, J. I. S. Angiotensin converting enzyme inhibitors and moderate hypertension. *Drugs* **1990**, *40*, 326−345.
(3) Greenlee, W. J. Renin Inhibitors. *Med. Res. Rev.* **1990**, *10*, 173−236.
(4) Wexler, R. R.; Greenlee, W. J.; Irvin, J. D.; Goldberg, M. R.; Prendergast, K.; Smith, R. D.; Timmermans, P. B. W. M. Nonpeptide Angiotensin II Receptor Antagonists: The Next Generation in Antihypertensive Therapy. *J. Med. Chem.* **1996**, *39*, 625−656.
(5) Judd, D. B.; Dowle, M. D.; Middlemiss, D.; Scopes, D. I. C.; Ross, B. C.; Jack, T. I.; Pass, M.; Tranquillini, E.; Hobson, J. E.; Panchal, T. A.; Stuart, P. G.; Paton, J. M. S.; Hubbard, T.; Hilditch, A.; Drew, G. M.; Robertson, M. J.; Clark, K. L.; Travers, A.; Donnelly, M. D.; Walker, D. G.; Richards, S. A. Bromobenzofuran-Based Non-peptide Antagonists of Angiotensin II: GR138950, a Potent Antihypertensive Agent with High Oral Bioavailability. *J. Med. Chem.* **1994**, *37*, 3108−3120.
(6) Mealy, N.; Castaner, J. Elisartan Potassium. *Drugs of the Future*, **1996**, *21*, 139−142.
(7) Kubo, K.; Kohara, Y.; Imamiya, E.; Sigiura, Y.; Inada, Y.; Furukawa, Y.; Nishikawa, K.; Naka, T. Nonpeptide angiotensin II receptor antagonists. Synthesis and biological activity of benzimidazolecarboxylic acids. *J. Med. Chem.* **1993**, *36*, 2182−2195.
(8) Stearns, R. A.; Miller, R. R.; Doss, G. A.; Chakravarty, P. K.; Rosegay, A.; Gatto, G. J.; Chiu, S.-H. L. The Metabolism of DuP753, a Nonpeptide Angiotensin II Receptor Antagonist, by Rat, Monkey, and Human Liver Slices. *Drug Metab. Dispos.* **1992**, *20*, 281−287.
(9) Sweet, C. S.; Nelson, E. B. How well have animal studies with losartan predicted responses in humans. *J. Hypertens.* **1993**, *11* (Suppl. 3), S63−S67.
(10) Wong, P. C.; Price, W. A.; Chiu, A. T.; Duncia, J. V.; Carini, D. J.; Wexler, R. R.; Johnson, A. L.; Timmermans, P. B. W. M. Nonpeptide Angiotensin II Receptor Antagonists. XI. Pharmacology of EXP3174: An Active Metabolite of DuP 753, An Orally Active Antihypertensive Agent. *J. Pharmacol. Exp. Ther.* **1990**, *255*, 211−217.
(11) Ellingboe, J. W.; Antane, M.; Nguyen, T. T.; Collini, M. D.; Antane, S.; Bender, R.; Hartupee, D.; White, V.; McCallum, J.; Park, C. H.; Russo, A.; Osler, M.; Wojdan, A.; Dinish, J.; Ho, D. M.; Bagli, J. F. Pyrido[2,3-*d*]pyrimidine Angiotensin II Antagonists. *J. Med. Chem.* **1994**, *37*, 542−550.
(12) Hultin, T. A.; Lihotz, L. A.; Scatina, J. Comparative Metabolism of Tasosartan in Mice, Rats, Dogs and Monkeys. *Int. Soc. Study Xenobiotics Proc.* **1997**, *11*, 226.
(13) Sakamoto, T.; Kondo, Y.; Yamanaka, H. Studies on Pyrimidine Derivatives. XXVIII. Synthesis of Pyridopyrimidine Derivatives by Cross-coupling of Halopyrimidines with Olefins and Acetylenes. *Chem. Pharm. Bull.* **1982**, *30*, 2410−2416.
(14) Underwood, D. J.; Strader, C. D.; Rivero, R.; Patchett, A. A.; Greenlee, W.; Prendergast, K. Structural model of antagonist and agonist binding to the angiotensin II, AT_1 subtype, G protein coupled receptor. *Chem. Biol.* **1994**, *1*, 211−221.
(15) Prendergast, K.; Adams, K.; Greenlee, W. J.; Nachbar, R. B.; Patchett, A. A.; Underwood, D. J. Derivation of a 3D pharmacophore model for the angiotensin-II site one receptor. *J. Comput.-Aided Mol. Des.* **1994**, *8*, 491−512.
(16) Sybyl, v6.4, Tripos Associates, St. Louis, Missouri.

JM970690Q